Effect of Fiber Orientation and Ply-Stacking Sequence on Buckling Behaviour of Basalt/Epoxy and Basalt-Carbon/Epoxy Composite Laminates

by

Salem Omar Abdullah Bin Dhuban

14633

Dissertation submitted in partial fulfilment of
the requirements for the
Bachelor of Engineering (Hons)
(Mechanical)

APRIL 2015

Universiti Teknologi PETRONAS
Bandar Seri Iskandar
31750 Tronoh
Perak Darul Ridzua

CERTIFICATION OF APPROVAL

Effect of Fiber Orientation and Ply-Stacking Sequence on Buckling Behaviour of Basalt/Epoxy and Basalt-Carbon/Epoxy Composite Laminates

by

Salem Omar Abdullah Bin Dhuban

14633

A project dissertation submitted to the
Mechanical Engineering Programme
Universiti Teknologi PETRONAS
in partial fulfilment of the requirement for the
BACHELOR OF ENGINEERING (Hons)
(MECHANICAL)

Approved by,

_____

(Dr. Saravanan Karuppanan)

UNIVERSITI TEKNOLOGI PETRONAS
TRONOH, PERAK
April 2015

CERTIFICATION OF ORIGINALITY

This is to certify that I am responsible for the work submitted in this project, that the original work is my own except as specified in the references and acknowledgements, and that the original work contained herein have not been undertaken or done by unspecified sources or persons.

_____

SALEM OMAR ABDULLAH BIN DHUBAN

ABSTRACT

Composite materials are materials that are made of two or more constituents. Each constituent has distinct properties. The two main constituents are reinforcement and matrix. Recently, the use of composite materials has increased rapidly due to their excellent mechanical properties such as high strength, low density, corrosion and fatigue resistance. Among the factors that affect the strength of composite materials are the mechanical properties of the reinforcement and matrix, orientation of the reinforcement and ply stacking sequence of the composite laminate. The main disadvantage of most of the reinforcement fibers such as carbon fiber and glass fiber is the high cost. Basalt fiber is a potential replacement for those materials as a reinforcement material. Basalt fiber showed mechanical properties similar to the mechanical properties of glass fiber but at affordable cost. The aims of this study are to investigate the effect of fiber orientation and ply-stacking sequence on the buckling behaviour of a symmetric basalt/epoxy and basalt-carbon/epoxy composite laminates using nonlinear finite element analysis (FEA) and experimentally. The effect of fiber orientation on the critical buckling load on basalt/epoxy was studied using four-layer symmetric laminated plate using the following orientations: $[\theta/90]_s^\circ$, $[90/\theta]_s^\circ$, $[\theta/0]_s^\circ$, $[0/\theta]_s^\circ$, $[30/\theta]_s^\circ$, $[\theta/30]_s^\circ$, $[30/\theta]_s^\circ$, $[\theta/45]_s^\circ$, $[45/\theta]_s^\circ$. The effect of ply-stacking sequence on the critical buckling load of eight-layer pure basalt/epoxy, carbon/epoxy and hybrid basalt-carbon/epoxy was investigated using the following stacking sequences: $[0_B/\ 0_B/\ 0_B/\ 0_B]_s^\circ$, $[0_C/\ 0_C/\ 0_C/\ 0_C]_s^\circ$, $[0_C/\ 0_C/\ 0_B/\pm 45_B]_s^\circ$, $[0_C/\ 0_C/\ \pm 45_B\ /0_B]_s^\circ$, $[0_C/\ 0_C/\ \pm 45_B/\ 0_C]_s^\circ$, $[\ 0_B/\pm 45_B/\ 0_C\ \ 0_C]_s^\circ$, $[\pm 45_B/0_B/\ 0_C/\ 0_C]_s^\circ$, $[\ 0_B/\ 0_C/\ 0_C/\pm 45_B]_s^\circ$, $[\pm 45_B/\ 0_C/\ 0_C/\pm 45_B]_s^\circ$. Experimental results had a good agreement with the nonlinear FEA results. Furthermore, it was found that the outer layers of the laminate sustain most of the load and laminates having 0° fiber orientation in the outer layers sustain higher buckling loads. Pure carbon/epoxy laminate have five times higher buckling load than that of pure basalt/epoxy. $[0_C/\ 0_C/\ 0_B/\pm 45_B]_s^\circ$ laminate is the best optimization of the hybrid stacking sequences as far as buckling strength is concerned.

ACKNOWLEDGEMENTS

I would like to express my sincere gratitude to my supervisor Dr. Saravanan Karuppanan for his supervision, monitoring, teaching, guidance and support. Special thanks go to Mr. Ali Nawaz for his guidance throughout the project period. Not forgetting to give a warm thanks to Mr. Santosh for his invaluable advices and comments that helped me achieve the project objectives successfully.

TABLE OF CONTENTS

LIST OF FIGURES

LIST OF TABLES

CHAPTER 1

INTRODUCTION

1.1 BACKGROUND OF THE STUDY

The use of composite materials is increasing rapidly in many applications. According to Campbell [1], composite material can be defined as a material that is made of two or more constituents having dissimilar physical properties. The mix of the constituents gives better properties than the individual material. Unlike metallic alloys, the physical, chemical and mechanical properties of each constituent of the composite laminate are retained. The two constituents are the reinforcement and matrix. The most obvious advantages of composites compared to the individual materials are strength, low density, corrosion resistance, the ability to orient the plies for maximum stiffness and strength, enhanced fatigue strength and reduced assembly costs. Therefore composite materials are being used in vast number of applications including structure of buildings, sports equipment, cars and even in aerospace industry [1].

The continuous phase of the composite is the matrix. Common matrix materials are polymer, ceramic and metals. The functions of the matrix are to distribute the load between the fibers, stabilize the fibers, act as a protective layer to protect the reinforcement from the environmental factors such as abrasion and corrosion. It also carries the interlaminar shear load which is the shear between two layers [1].

The reinforcement provides stiffness and strength to the composite. There are two main types of reinforcement, fiber and particle reinforcement. Fiber reinforced composite are generally stiffer and stronger than particulate reinforced composites. Fiber reinforced composites are limited to a content of 70 % of fibers. At higher values of the reinforcement the matrix will be too weak to support the reinforcement. Common fibers are carbon fibers, glass fibers, Kevlar fibers and basalt fibers [1].

1.1.1 Laminates

According to Campbell [1] multiple plies stacked together in one direction is called lamina (Fig. 1.1a). On the other hand, multiple plies arranged in different directions is called laminate (Fig. 1.1b). Continuous reinforcements are usually arranged as a laminate material. Fiber laminates are arranged in a way that improves the strength in certain direction. Unidirectional ply arrangement (0°) has very high strength and stiffness in the in-plane direction (0°) but the strength in the normal direction (90°) is low because the load is sustained by the weak matrix. Fiber orientation is the primary determinant of the load carrying capability of laminates. It is important to orient the fibers in a way that enhances the laminate strength in a certain direction to cope with the load type. While this approach is effective in the case of unidirectional load, some laminates are subjected to different types of load; therefore it is necessary to find the balanced fiber orientation for a better load carrying capability in different directions. This may be done by orienting each ply of the laminate in different fiber orientation such as $[0, +45, -45, 90]^{\circ}$ [1].

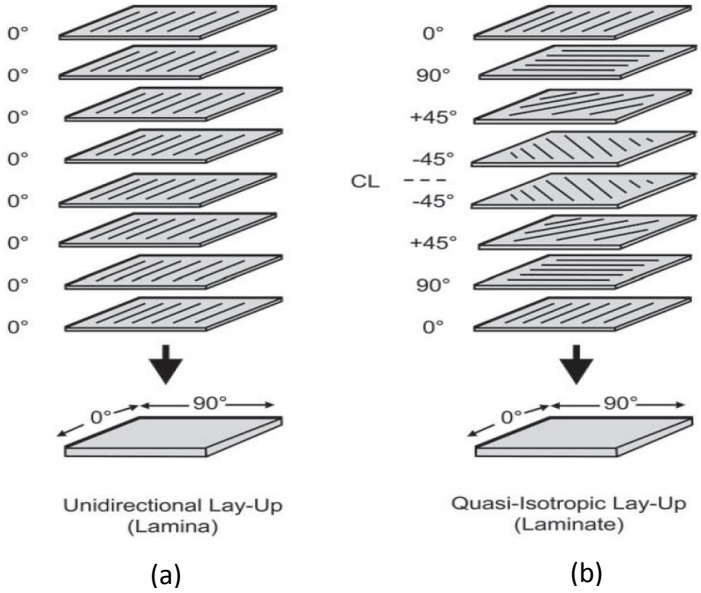

Figure 1.1 Lamina and laminate lay-ups [1]

1.2 PROBLEM STATEMENT

As the use of composite materials increases, it became a necessity to optimize the performance of those materials and predict its behaviour under various loading and working conditions. Numerous studies have been done to investigate the behaviour of those materials, including buckling behaviour, effect of fiber orientation and ply-stacking sequence on the critical buckling load of many composite laminates such as glass/epoxy laminate. Basalt fiber is a relatively new material where the effect of fiber orientation and ply-stacking sequence on the buckling behaviour of basalt/ epoxy has not been studied. Therefore, studying the effect of fiber orientation and ply-stacking sequence on the buckling behaviour of basalt/epoxy will be a good contribution.

1.3 OBJECTIVES

The aims of this study are:

1. To investigate the effect of fiber orientation on the buckling behaviour of basalt/epoxy composite laminates using nonlinear FEA.
2. To study the effect of ply stacking sequence on the buckling behaviour of basalt-carbon/epoxy composite laminates using nonlinear FEA.
3. To compare the FEA results with the experimental results.

1.4 SCOPE OF THE STUDY

The buckling behaviour of basalt/epoxy and hybrid basalt-carbon/epoxy composite laminates will be investigated in this study. To conduct the study, laminates will be subjected to specific conditions such as:

1. Uniaxial compressive load.
2. SFSF boundary conditions, where S= simply supported edge, F= free edge.
3. Constant aspect ratio.
4. Constant laminate thickness.
5. Constant fiber content.

CHAPTER 2

LITERATURE REVIEW

The light weight and good mechanical properties of composite laminates made it preferable for many applications. Load carrying behaviour of composite laminates depends very much on the load direction and fiber orientation of the laminates [2]. Composite laminates show totally different resistance to load applied normal to the fiber orientation than load applied in the direction of the fibres [1]. Throughout the years there have been numerous studies to investigate the effect of different parameters on the behaviour of composite laminates.

The mechanical properties of composite laminates are affected by many parameters such as fiber type, matrix type, fiber orientation, ply stacking sequence, laminate thickness, aspect ratio, boundary conditions, delamination size and temperature. Alam *et al.* [3] reported that fiber orientation does not affect the hardness of glass reinforced polymers (GRP) and it has small effect on the density and impact strength, but fiber orientation has significant effect on the tensile strength of GRP.

One of the most critical failure modes of composite laminates is buckling failure. Buckling can occur at loads lower than the strength limit and it results in large deformation of the structure [2]. Jiangbo and Junjiang [4] investigated the effect of temperature on the critical buckling load of ultra-thin-walled lenticular collapsible composite tube (LCCT) subjected to axial compression load. The experiment was conducted at -80°C, 25°C and 100°C. Results showed that low temperature has positive effect on the critical buckling load of thin composite tubes. Buckling load at -80°C is 2.2% higher than buckling load at 25°C. Meanwhile, buckling load at 100°C is 19.5% lower than that at 25°C.

Critical buckling loads of composite laminates are influenced by many factors such as fiber orientation, ply stacking sequence, boundary conditions, aspect ratio, thickness of the laminates, stiffening type, loading condition and number of layers of the laminate. Shukla *et al.* [5] concluded that buckling strength of laminated plate is significantly influenced by material properties such as modulus of elasticity, plate aspect ratio and stacking sequence.

Critical buckling load is significantly affected by mixed boundary conditions [6]. Stiffened composite laminate panels sustain higher buckling load than unstiffened panels as reported by SudhirSastry *et al.* [7]. Nevertheless, Guo *et al.* [8] reported that critical buckling load of stiffened panels is enhanced by the depth of the stiffener but only to a certain value. Short *et al.* [9] investigated the effect of delamination in curved and flat composite laminates under compression loading and showed that critical buckling load of curved laminates is less than the critical buckling load of flat laminates. Moreover, as the delamination moves to the outside of the curve the strength reduction increases. In contrast to the buckling load, the critical delamination diameter is not affected by fiber orientation of the laminated composite [10].

Another important variable in the critical buckling load is the aspect ratio of the laminate. Maximum buckling load tends to decrease with increasing aspect ratio [6, 11-13]. Furthermore, Ni *et al.* [14] reported that maximum buckling load tends to decrease with increasing aspect ratio of short plates but in the case of long plates the effect of aspect ratio is negligible. Besides that, number of plies influences the buckling load of the laminate as suggested by Park *et al.* [15]. Number of plies has positive effect on load carrying capability of laminates with aspect ratio $a/b = 1$ under transverse load, but the effect of number of plies for laminates under in-plane load is negligible. Topal and Uzman [16] reported that the number of layers in the composite laminates gradually increases the maximum buckling load for symmetric laminates, while in the case of asymmetric laminates there is a rapid increase of the maximum buckling load from two to four layers, and after that the rate is slow. Analytical and FEA results showed that, asymmetric rectangular laminates have higher critical buckling load than that of symmetric specimens [17].

Cagdas and Adali [18] studied the optimum design of a simply supported variable curvature laminated angle-ply composite panel under uniaxial compression and concluded that thick angle-ply curvature laminate panels under uniaxial compression load fails because of the first-ply failure rather than buckling failure, but for thin laminates the dominant failure mode is due to buckling failure. There exists a minimum thickness at which the dominant failure mode is buckling, beyond that thickness, laminates fail due to first-ply failure [18].

Several studies have been conducted to investigate the effect of fiber orientation and ply stacking sequence on the buckling behaviour of laminated composites. Optimum buckling strength of laminated fiber composite cylinders under compression load is affected not only by fiber orientation but also by ply stacking sequence [19]. Topal [20] investigated the optimum fiber orientation, aspect ratio and boundary conditions of six-layer laminate subjected to biaxial load and simply supported boundary conditions. The optimization was done using layer wise optimization theory. The optimum fiber orientation was found to be $[90/90/90/90]^{\circ}$ for all aspect ratios. On the other hand $[0/0/0/0]^{\circ}$ orientation was found to be the best orientation for all boundary conditions [20]. The optimum fiber orientation of four-ply simply supported rectangular laminate plate with aspect ratio *a/b* = 3 under uniaxial compression load is $[45/-45]_s^{\circ}$ [21].

Jadhav and Gunjavate [22] investigated the maximum buckling load of fiberglass laminates. FEA using ANSYS was utilized. It was reported that laminates having 0° fiber orientation in the outer surface sustain higher buckling loads than laminates with 90° orientation in the outer surface and symmetric laminates of five layers sustained higher buckling load compared to asymmetric laminates [22].

Heidari-Rarani *et al.* [2] investigated the ply stacking sequence on the buckling behaviour of E-glass epoxy using analytical, numerical and experimental methods. First, the effect of ply stacking was investigated using semi numerical approach based on Rayleigh Ritz method. Calculations were performed on four layers laminate arranged in cross-ply and angle-ply orientation with boundary condition SFSF (S= simple support, F = free support). The laminate was subjected to axial compression load. Then, buckling analysis of the laminate under the same condition was performed using numerical simulation via ABAQUS software. Failure criterions used in the analysis were Hashin, Tsai-Wh and Tsai Hill. To validate the results of the analytical and numerical approaches three different orientations were investigated experimentally. It was found that the buckling load of $[90/0]_s^{\circ}$ is half the buckling load of $[0/90]_s^{\circ}$.

Wind turbine blades are designed to meet several major structural conditions, including tip deflection, strength and buckling. Blades are primarily made of GRP, which is expected to continue while carbon fiber reinforcements are being introduced

into blades. Carbon fiber reinforcements can be used to improve the stiffness and tensile strength in the fiber direction, as compared to materials containing glass, but the gains in compressive strength are generally significantly lower. Proper selection of ply orientation in advanced composite materials is necessary to provide a structurally efficient design. The part might require 0° plies to react to axial loads, $\pm 45^{\circ}$ plies to react to shear loads and 90° plies to react to side loads [23].

Many of the studies compared experimental results with FEA results. Boni *et al.* [24] studied the post-buckling behaviour of flat stiffened composite panels under compressive load using experimental and FEA approaches. Results indicated that maximum displacement obtained by both methods is closely matched, but there are some differences in the buckles shapes. Strain values of the experiment are slightly lower than those of the FEA approach [24]. Experimental results were compared to ANSYS FEA results; both methods gave close estimation of the critical buckling load [10, 24].

The objective of the current study is to investigate the effect of fiber orientation on the critical buckling load of a symmetric basalt/epoxy composite laminated plate and a symmetric hybrid basalt-carbon/epoxy composite laminated plate under uniaxial compressive load and simply supported boundary conditions. The study will be done using two methods, nonlinear FEA using ANSYS and experimental method.

CHAPTER 3

METHODOLOGY

Buckling behaviour of a symmetric basalt/epoxy and basalt-carbon/epoxy hybrid composite laminated plate were investigated using nonlinear FEA and experimentally. The specimen dimensions are 400 mm × 40 mm × 3.2 mm in length, width and thickness, respectively. Two edges of the specimen were simply supported and the other two were left free. Figure 3.1 and 3.2 show the meshed FEA model and experimental specimen, respectively.

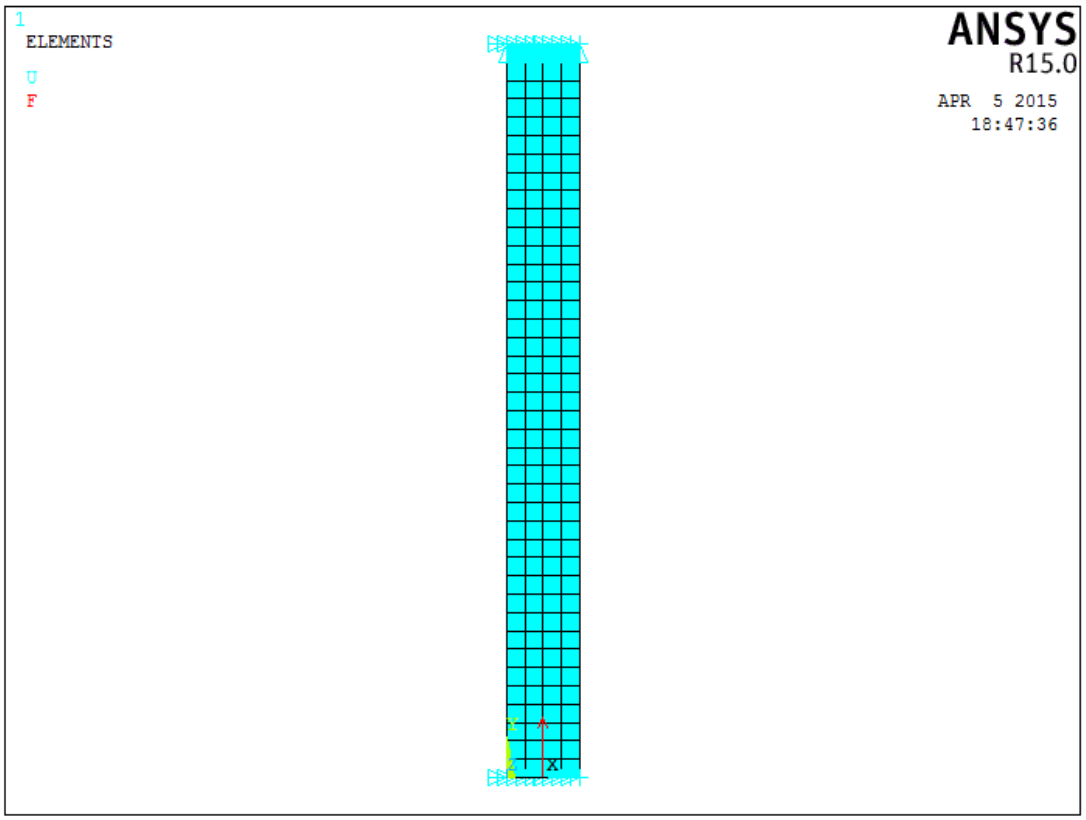

Figure 3.1 Meshed FEA model

Figure 3.2 Experimental specimen

3.1 NUMERICAL AND EXPERIMENTAL RESULTS COMPARISON

Six different laminates were studied using FEA and experimentally. The results of both methods were compared to validate the results of the FEA. The six laminates are:

$[0_B/\ 0_B/\ 0_B/\ 0_B]_S^\circ$, $[0_C/\ 0_C/\ 0_B/\pm 45_B]_S^\circ$, $[0_C/\ 0_C/\pm 45_B\ /0_B]_S^\circ$, $[\pm 45_B/0_B/\ 0_C/\ 0_C]_S^\circ$, $[0_C/\ 0_C/\ \pm 45_B/\ 0_C]_S^\circ$, $[\pm 45_B/\ 0_C/\ 0_C/\pm 45_B]_S^\circ$.

3.2 EFFECT OF FIBER ORIENTATION

To study the effect of fiber orientation on the critical buckling load of basalt/epoxy composite laminated plate, the following layups were used:

$[\theta/90]_S^\circ$, $[90/\theta]_S^\circ$, $[\theta/0]_S^\circ$, $[0/\theta]_S^\circ$, $[\theta/30]_S^\circ$, $[30/\theta]_S^\circ$, $[\theta/45]_S^\circ$, $[45/\theta]_S^\circ$

Θ layer was varied from $0^{\circ} - 90^{\circ}$ while keeping the other layers constant. Figure 3.3 shows the stacking sequence of $[90/90]_s^{\circ}$ laminate.

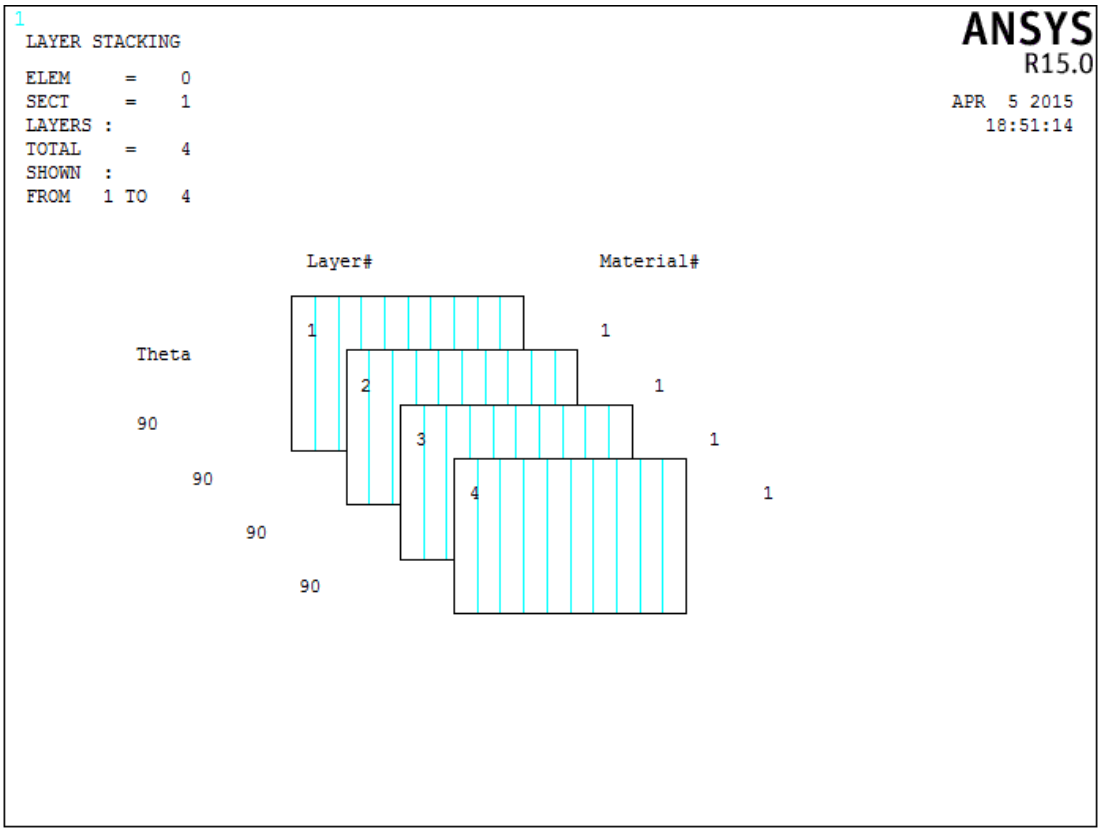

Figure 3.3 Stacking sequence of $[90/90]_s^{\circ}$ laminate

3.3 EFFECT OF PLY-STACKING SEQUENCE

The effect of the ply stacking sequence on the critical buckling load of basalt-carbon/epoxy hybrid composite laminates was studied using nonlinear FEA. The following laminates were used in the study:

$[0_C/\,0_C/\,0_B/\pm 45_B]_s^{\circ}$, $[0_C/\,0_C/\pm 45_B\,/0_B]_s^{\circ}$, $[\pm 45_B/0_B/\;0_C/\,0_C]_s^{\circ}$, $[0_C/\,0_C/\,\pm 45_B/\,0_C]_s^{\circ}$, $[\pm 45_B/\,0_C/\;0_C/\pm 45_B]_s^{\circ}$, $[0_C/\,0_C/\,0_C/\,0_C]_s^{\circ}$, $[0_B/\,0_B/\,0_B/\,0_B]_s^{\circ}$, $[\,0_B/\pm 45_B/\,0_C\;\;0_C]_s^{\circ}$, $[\,0_B/\,0_C/\;\;0_C/\pm 45_B]_s^{\circ}$.

Where:

0°_{C}: Carbon fiber reinforced layer in 0° direction.

0°_{B}: Basalt fiber reinforced layer in 0°direction.

$\pm 45^{\circ}_{B}$: Woven basalt fiber reinforced layer in $\pm 45^{\circ}$direction.

3.4 EXPERIMENTAL PROCEDURE

3.4.1 Sample Preparation

3.4.1.1 Materials and tools required

The Materials and tools that are required for the preparation of composite laminates using hand layup method are illustrated below:

1. A mold.
2. Gel coating.
3. Epoxy resin and hardener.
4. Basalt fibers and carbon fibers.
5. Cutting and mixing tools.
6. Impregnation tools such as brushes rollers and Squeegees.

3.4.1.2 Procedure

The procedure of preparing composite laminates using hand layup method is illustrated below:

1. The mold is cleaned to remove all left over from previous molding processes.
2. A release agent is applied to the mold surface.
3. The surface layer (“gel coat”) is applied to the mould surface.
4. The epoxy is mixed.
5. The surface layer is primed using epoxy to promote bonding between the surface layer and the fibres.

6. The first layer of fibers is laid.
7. The reinforcing fibres are layered one on top of the other according to the lay-up schedule. The layers should be laid wet in wet; this means that consecutive layers are laid on top of the others before the epoxy has gelled to promote bonding between the layers.
8. After the final layer of fibre has been applied a layer of peel ply is applied on the surface.
9. The part is cured at room temperature.
10. The part is de-moulded.

3.4.2 Buckling Experiment

The experiment was performed using strut buckling apparatus. Figure 3.4 shows the strut buckling apparatus. The experimental procedure is illustrated below:

1. The theoretical buckling load was calculated using linear FEA.
2. The simply supported edges was fixed in the apparatus.
3. The load indicator was set to zero by pressing "TARE" button.
4. The specimen was fixed in the apparatus. It is important that the reading shown by the load indicator is less than 10 N.
5. The dial gauge was fixed at the mid-length of the strut and set to zero.
6. The load indicator was set to zero again.
7. The specimen was loaded at suitable increments.
8. The load and the corresponding mid-length deflection were recorded.
9. The best fit line of the deflection (d) versus deflection over load (d/p) was plotted. The slop of the line represents the critical buckling load of the specimen.

Figurer 3.5 shows the deflection (d) vs deflection-load ratio (d/p) best fit line of $[0_C/\,0_C/\,0_B/\pm 45_B]_S^\circ$ laminate. The slop of the best fit line (628.98) is the critical buckling load in Newton.

Figure 3.4 Strut buckling apparatus

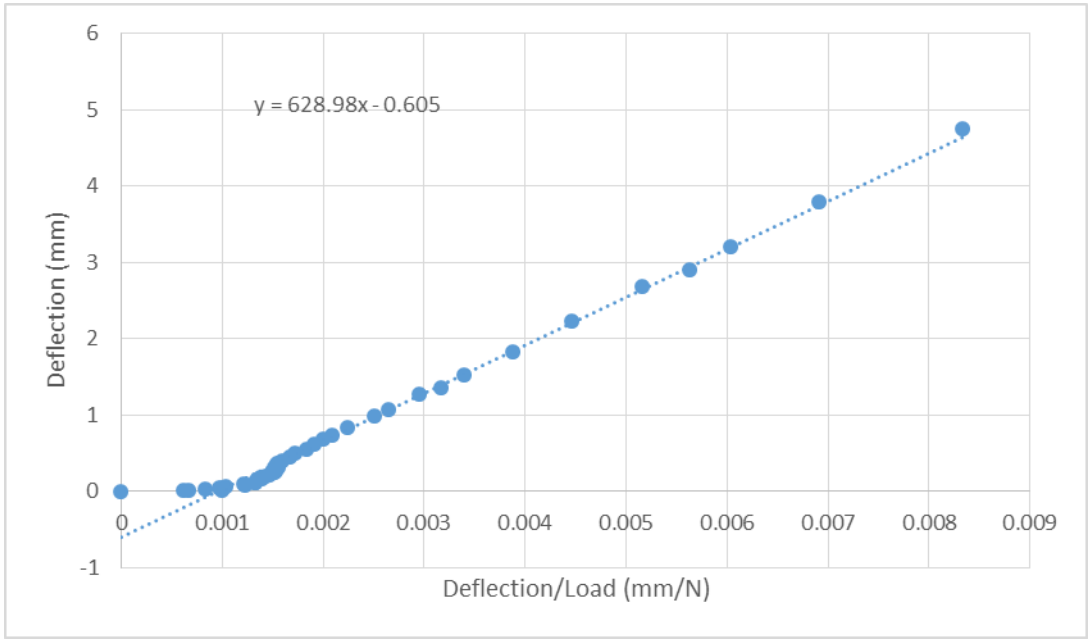

Figure 3.5 Deflection vs deflection-load ratio of $[0_C/\ 0_C/\ 0_B/\pm 45_B]_s^\circ$ laminate

3.5 FINITE ELEMENT ANALYSIS USING ANSYS

3.5.1 Element Type

SHELL281 element was used in the FEA. SHELL281 element is suitable for analysing thin to moderately-thick shell structures. The element has 8 nodes with 6 degrees of freedom at each node: translations in the x, y and z axes and rotations about the x, y and z axes. It is also suitable for large strain nonlinear analyses. Furthermore, it supports modelling of composite shells [26].

3.5.2 Linear Buckling Analysis Procedure Using ANSYS

The main steps of performing buckling analysis using ANSYS FEA package are illustrated below:

3.5.2.1 Preprocessor

1. Choose menu path **Main Menu> Preprocessor> Element Type> Add/Edit/Delete**. The Element Types dialog appears.
2. Click **Add** ... The Library of Element Types dialog appears.
3. In the scroll box on the left, select "Shell**".**
4. In the scroll box on the right, click "3-D 8node281**".**
5. Click **OK**, and then click **Close** in the Element Types dialog.
6. Define material properties. Choose menu path **Main Menu> Preprocessor>Material Props>Material Models**. The Define Material Model Behavior dialog appears.
7. In the Material Models Available window on the right, double-click the following: **Structural**, **Linear**, **Elastic**, **Orthotropic**. A dialog appears.
8. Enter the material properties. Table 3.1 shows the orthotropic properties of basalt fiber reinforced epoxy and carbon fiber reinforced epoxy.

Table 3.1 Mechanical properties of basalt/epoxy and carbon/epoxy lamina [25]

	Basalt/Epoxy	Carbon/Epoxy
Elastic Modulus, E_x (GPa)	30.2	74.7
Elastic Modulus, E_y (GPa)	5.2	4.7
Elastic Modulus, E_z (GPa)	5.2	4.7
Poisson's ratio, υ_{xy}	0.2	0.48
Poisson's ratio, υ_{yz}	0.21	0.47
Poisson's ratio, υ_{xz}	0.21	0.47
Rigidity Modulus, G_{xy} (GPa)	2.05	21.5
Rigidity Modulus, G_{yz} (GPa)	3.6	1.45
Rigidity Modulus, G_{xz} (GPa)	3.6	21.5

9. Choose menu path **Material> Exit** to close the Define Material Model Behavior dialog.
10. Define ply stacking sequence. Choose menu path **Main Menu> Preprocessor> Section> Shell> Lay Up > Add/Edit.** Create and Modify Shell Section dialog appears.
11. Specify number of layers, layer thickness and fiber orientation of each layer, and click **OK.**
12. Create the model. Choose menu path **Main Menu> Preprocessor> Modelling> Create> Area> Rectangular> By Dimensions**. Create Rectangular by Dimensions dialog appears.
13. Enter 0, 40 in X1, X2 fields. Enter 0, 400 in Y1, Y2 fields. Click **OK**.
14. Define number of divisions. Choose menu path **Main Menu> Preprocessor> Meshing> Mesh too**l. In the Size Control Section, click Set next to lines. The Element Size on Picked dialog appears. Pick the right and left lines and click **OK**. Enter 40 in the "No. of Element Divisions" field and click **Apply**.
15. Pick the bottom and upper lines and click **OK**. Enter 4 in the "No. of Element Divisions" field and click **OK**.
16. Click **mesh** in the Mesh Tool. Pick the area and click **OK**.
17. Click **Close** on the Mesh Tool.

3.5.2.2 Solution

1. Define boundary conditions. Choose menu path **Main Menu> Solution> Define Loads>Apply> Structural> Displacement> On Nodes**. The Apply U, ROT on KPs picker appears.
2. Select the upper nodes and click **Apply**. The Apply U, ROT on KPs dialog appears.
3. Select UX, UY and UZ to be constrained and enter 0 in the "Displacement Value" field.
4. Select the lower nodes and click ok. The Apply U, ROT on KPs dialog appears.
5. Select UX and UZ to be constrained and enter 0 in the "Displacement Value**"** field.
6. Apply force in the middle node of the bottom line. Choose menu path **Main Menu> Solution> Define Loads> Apply> Structural> Force/Moment> On Nodes**.
7. The Apply F/M on KPs picker appears. Pick the middle node of the bottom line and click **OK**.
8. In the drop down list for Direction of force/mom, select **FY**.
9. Enter 1 for the Force/Moment value in the Apply F/M on KPs dialog, and click **OK**.

3.5.2.3 Solve the Eigenvalue Buckling Analysis

1. Set analysis options. Choose menu path **Main Menu> Solution> Unabridged Menu> Analysis Type>Analysis Options**. The Static or Steady-State Analysis dialog appears.
2. Use the Sparse solver for the solution. In the Static or Steady-State Analysis dialog, make sure that Sparse solver is selected in the drop down box beside the Equation solver label.
3. Include Prestress effect, which will be stored for later use in the eigenvalue buckling calculation. In the drop down list labeled Stress stiffness or prestress, select "Prestress ON". Click **OK** to close the Static or Steady-State Analysis dialog.

4. Choose menu path **Main Menu> Solution> Solve> Current LS**. Click **OK** in the Solve Current Load Step window to begin the solution.
5. When the Solution is Done! window appears, click **Close** to close it.
6. Choose menu path **Main Menu> Finish**.
7. Choose menu path **Main Menu> Solution> Analysis Type> New Analysis**
8. Select the "Eigen Buckling" option, then click **OK**.
9. Choose menu path **Main Menu> Solution> Analysis Type> Analysis Options**. The Eigenvalue Buckling Options dialog appears. Select the “Block Lanczos” option. Enter 4 in the “No. of modes to extract” field, then click **OK**.
10. Set the element calculation key for the “MXPAND” command. Choose menu path **Main Menu> Solution>Load Step Opts> ExpansionPass> Single Expand> Expand Modes**.
11. In the Expand Modes dialog, enter 4 in the “No. of modes to expand” field, change the “No” to “Yes” beside the “Calculate elem results” label, and click **OK**.
12. Choose menu path **Main Menu> Solution> Solve> Current LS**. Click **OK** in the Solve Current Load Step window to begin the solution.
13. When the Solution is Done! window appears, click Close to close it.

3.5.2.4 Post Processor

1. Display the results summary. Choose menu path **Main Menu> General Postproc> Results Summary**.
2. Choose menu path **Main Menu> General Postproc> Read Results> First Set**.
3. Plot the first mode shape of the element. Choose menu path **Main Menu> General Postproc> Plot Results>Deformed Shape**. The Plot Deformed Shape dialog appears. Select “Def shape only” and click **OK**.
4. Choose menu path **Main Menu> Finish**.

For faster analysis ANSYS command can be used to perform the analysis. **See Appendix A** for more information about ANSYS command code of this analysis. Figure 3.6 shows the first buckling mode of $[90/90]_s^\circ$ laminate.

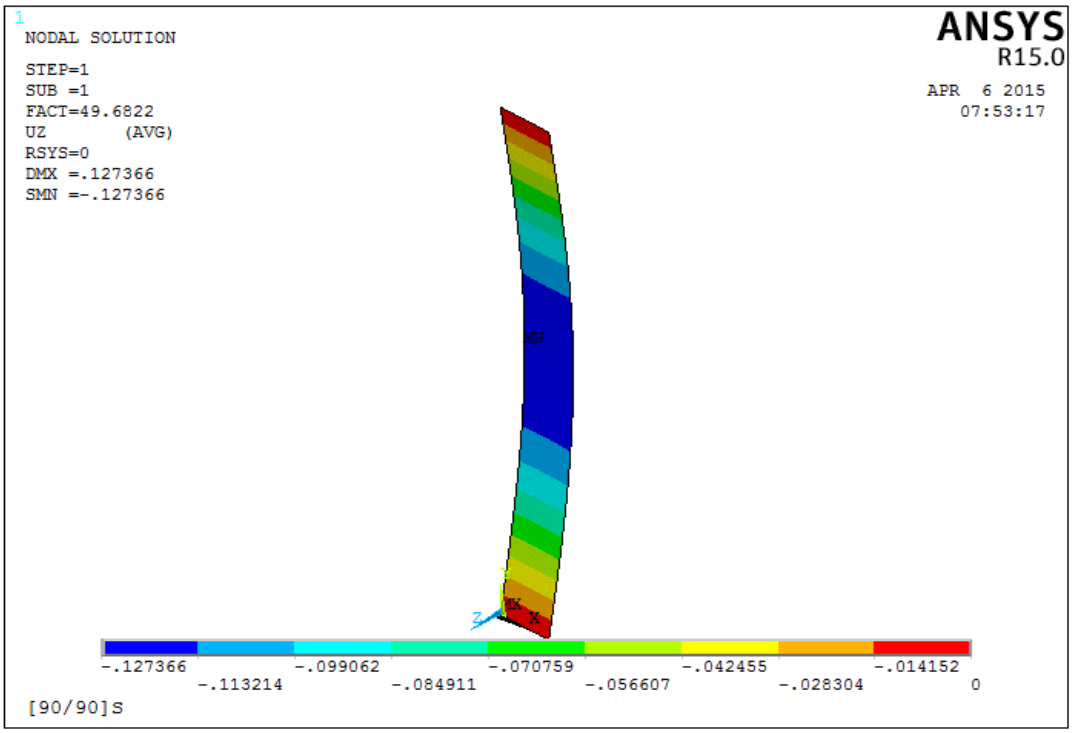

Figure 3.6 First buckling mode of $[90/90]_s^\circ$ laminate

3.5.3 Nonlinear Buckling Analysis Procedure Using ANSYS

1. Introduce model imperfections calculated by the previous analysis. Choose menu path **Main Menu> Preprocessor> Modeling> Update Geom**. In the Update nodes using results file displacements dialog, enter 0.32 in the "Scaling factor" field, 1 in the "Load step" field, 1 in the "Substep" field, and file in the "Selection" field. Click **OK**.
2. Choose menu path **Main Menu> Solution> Analysis Type> New Analysis.**
3. Apply force in the middle node of the bottom line. The load applied should be slightly larger the critical buckling load that was predicted by the linear FEA. Choose menu path **Main Menu> Solution> Define Loads> Apply> Structural> Force/Moment> On Nodes.**

4. The Apply F/M on KPs picker appears. Pick the middle node of the bottom line and click **OK**.
5. In the drop down list for Direction of force/mom, select FY.
6. Choose menu path **Main Menu> Solution> Analysis Type> Sol'n Controls**. Select Large Displacement Static in the dropdown list in the Analysis Options section.
7. Enter 40 in the "Number of Substeps" field.
8. In the opened Solution Controls dialog, select Advance NL.
9. Set the arc-length method. In the Arc-length options section, select the radio button beside "Activate Are-length method" field. Enter 3 in the "Max multiplier" field and 0.003 in the "Min multiplier" field, and then click **OK**.
10. Solve the current model. Choose menu path **Main Menu> Solution> Solve> Current LS.**

3.5.3.1 Plot and Review the Results

1. Define the load point deflection to be read from the results file. Choose menu path **Main Menu> TimeHistPostPro>**, select Add button on the top left corner of the Defined Time-History Variables dialog.
2. The Add Time-History Variable dialog appears. Select **DOF Solution> Z-Component of displacement.**
3. The Node for Data dialog appears. Type 373 (the middle node number), and click **OK**.
4. Plot the graph of the load vs. displacement. Click on Graph Data button on the top left corner of the Defined Time-History Variables dialog.

Figure 3.7 shows the nonlinear value (displacement) vs. time (load) curve of $[0_C/\ 0_C/\ 0_B/\pm 45_B]_s$ laminate. The Y axis (value) represents the displacement and the X axis (time) represents the fraction of the applied load. In this case the applied load was 610 N. The point on the curve where a small increase in the load results in large deformation represents the buckling point. The critical buckling load is calculated by multiplying the time fraction (load) by the applied load. The graph shows that the critical time fraction is 0.93.

$$P_{cr} = 0.93 \times 610 = 567 \text{ N}$$

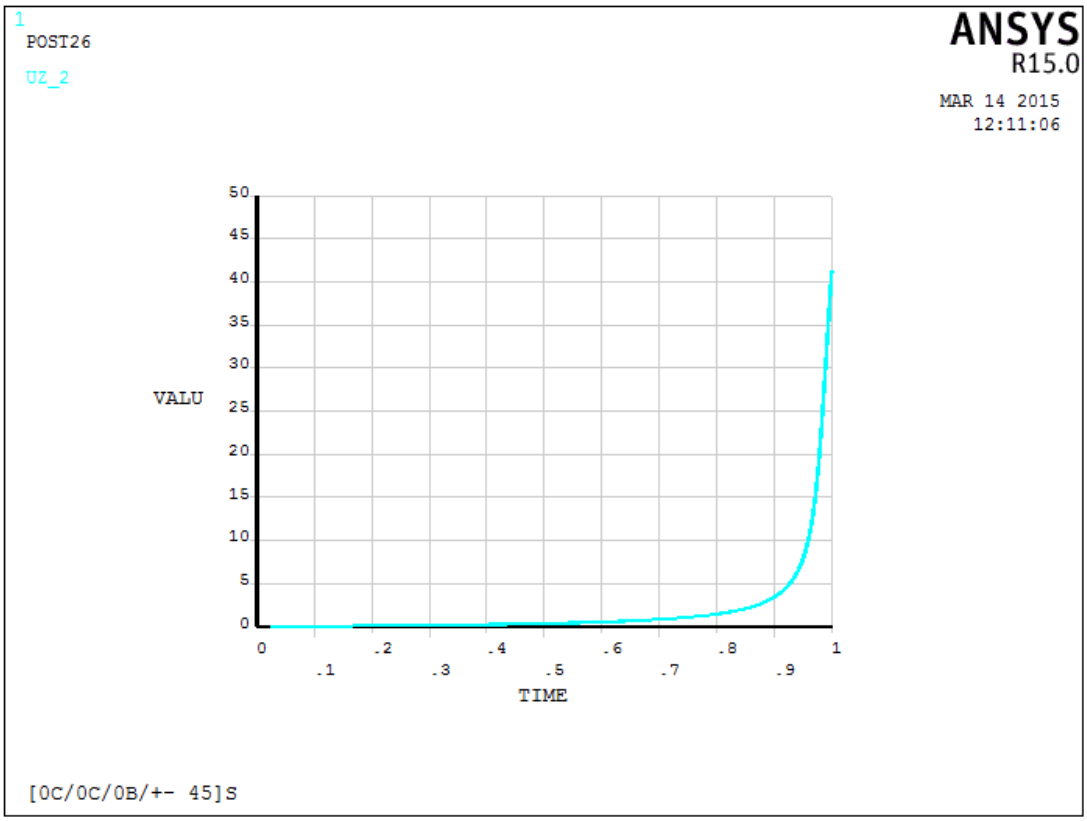

Figure 3.7 Nonlinear displacement vs load curve of $[0_C/\ 0_C/\ 0_B/\pm 45_B]_S^\circ$ laminate

3.6 KEY MILESTONE AND GANTT CHART

Table 3.2 and 3.3 show the key milestone and Gantt chart of FYP I and FYP II, respectively.

Table 3.2 Gantt chart of FYP I

Item/ Week (FYP1)	1	2	3	4	5	6	7	8	9	10	11	12	13	14
Project title selection														
Preliminary research and scope determination														
Literature review														
Extended proposal submission						*								
Studying finite element analysis														
Proposal defence									*					
Studying ANSYS software														
Submission of FYP1 draft report													*	
Submission of FYP1 interim report														*

Table 3.3 Gantt chart of FYP II

Item/ Week (FYP2)	1	2	3	4	5	6	7	8	9	10	11	12	13	14	15
Linear buckling analysis using ANSYS															
Nonlinear bucklingt analysis using ANSYS															
Preparation of the specimens															
Conducting the experiment															
Progress report submission							*								
Pre-EDX presentation										*					
Writing the final report															
Draft report submission													*		
Final report submission														*	
Viva															*

CHAPTER 4

RESULTS AND DISCUSSION

4.1 EXPERIMENTAL RESULTS

Experiments were conducted to study the critical buckling load of the following laminates:

$[0_B/\ 0_B/\ 0_B/\ 0_B]_s^\circ$, $[0_C/\ 0_C/\ 0_B/\pm 45_B]_s^\circ$, $[0_C/\ 0_C/\pm 45_B\ /0_B]_s^\circ$, $[0_C/\ 0_C/\ \pm 45_B/\ 0_C]_s^\circ$, $[\pm 45_B/0_B/\ 0_C/\ 0_C]_s^\circ$, $[\pm 45_B/\ 0_C/\ 0_C/\pm 45_B]_s^\circ$, $[\pm 45_B/\ 0_C/\ 0_C/\ 0_B]_s^\circ$.

The experimental results will be compared with the nonlinear FEA results of the exact dimensions of these laminates in section **4.2**.

Figure 4.1 through Figure 4.6 show deflection (d) vs deflection-load ratio (d/p) of the different laminates. The slop of the best fit line that are shown represents the critical buckling load.

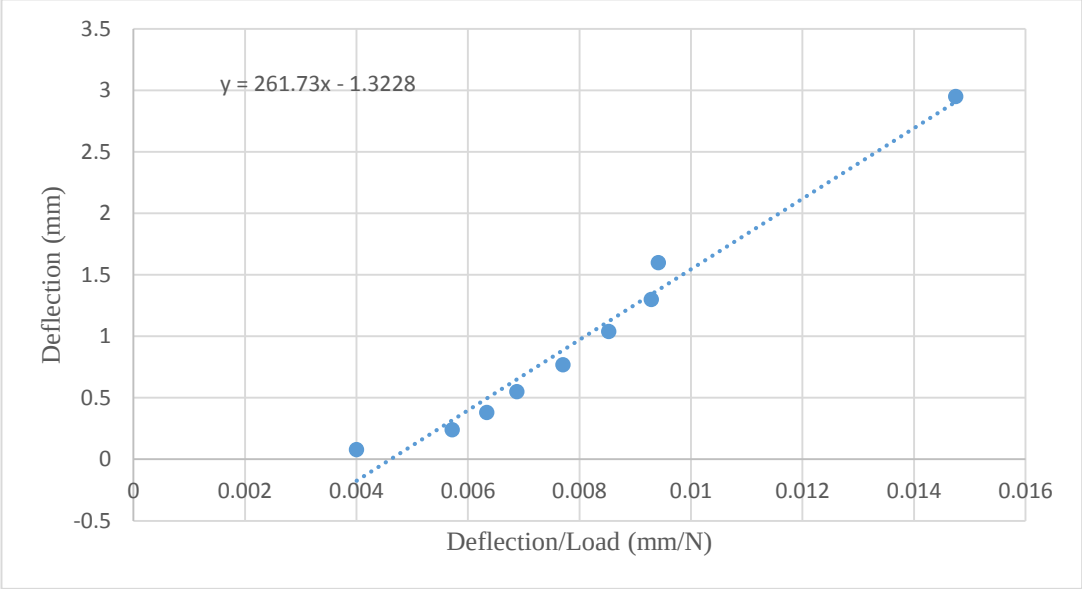

Figure 4.1 Deflection vs deflection-load ratio of $[0_B/\ 0_B/\ 0_B/\ 0_B]_s^\circ$ laminate

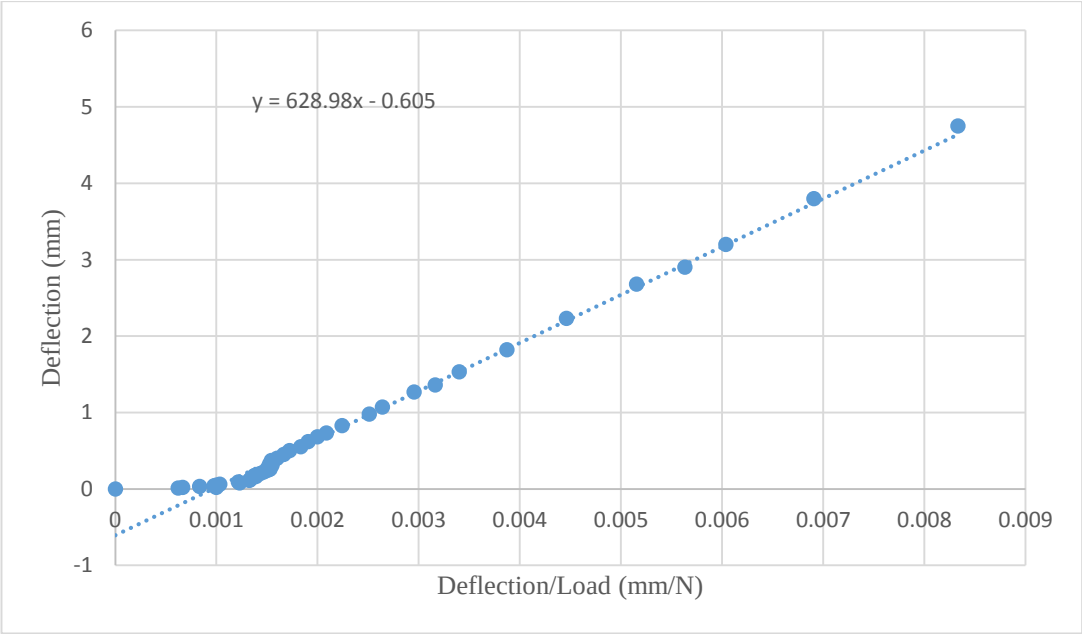

Figure 4.2 Deflection vs deflection-load ratio of $[0_C/\ 0_C/\ 0_B/\pm 45_B]_s^\circ$ laminate

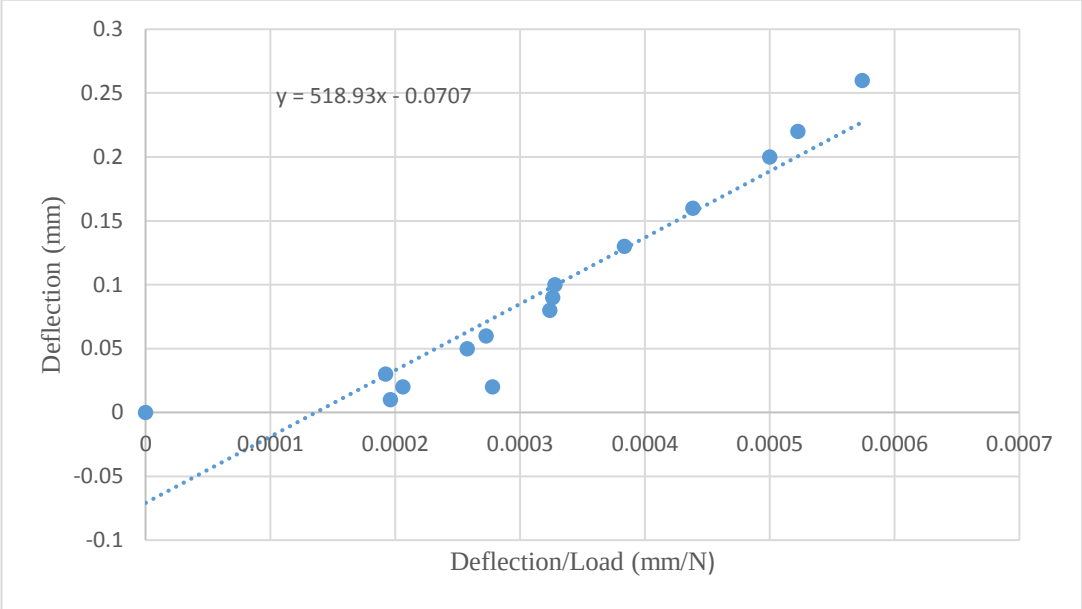

Figure 4.3 Deflection vs deflection-load ratio of $[0_C/\ 0_C/\pm 45_B\ /0_B]_s^\circ$ laminate

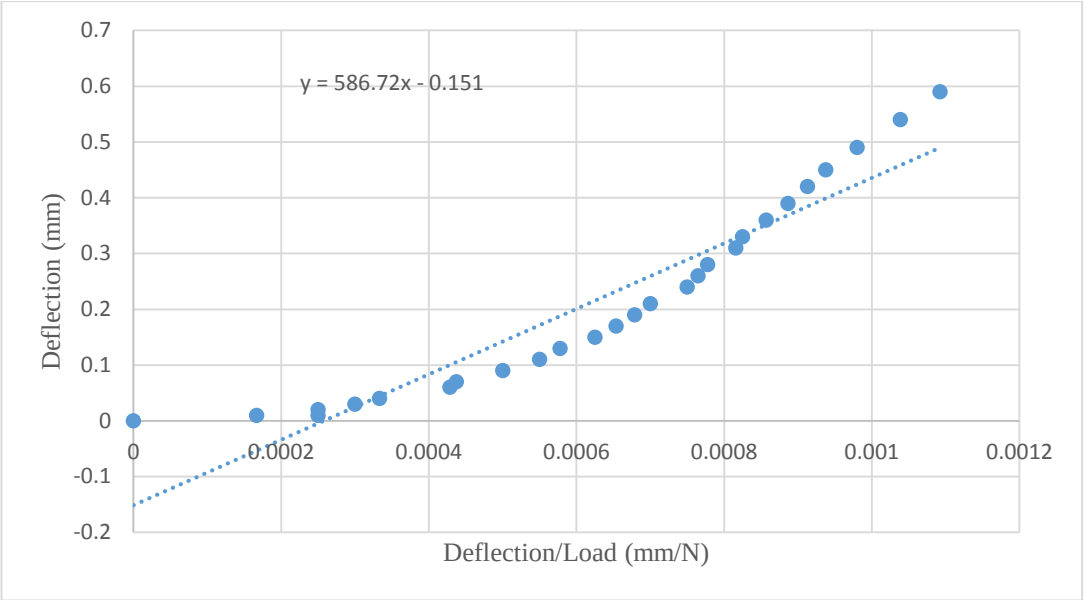

Figure 4.4 Deflection vs deflection-load ratio of $[0_C/\ 0_C/\ \pm 45_B/\ 0_C]_s^\circ$ Laminate

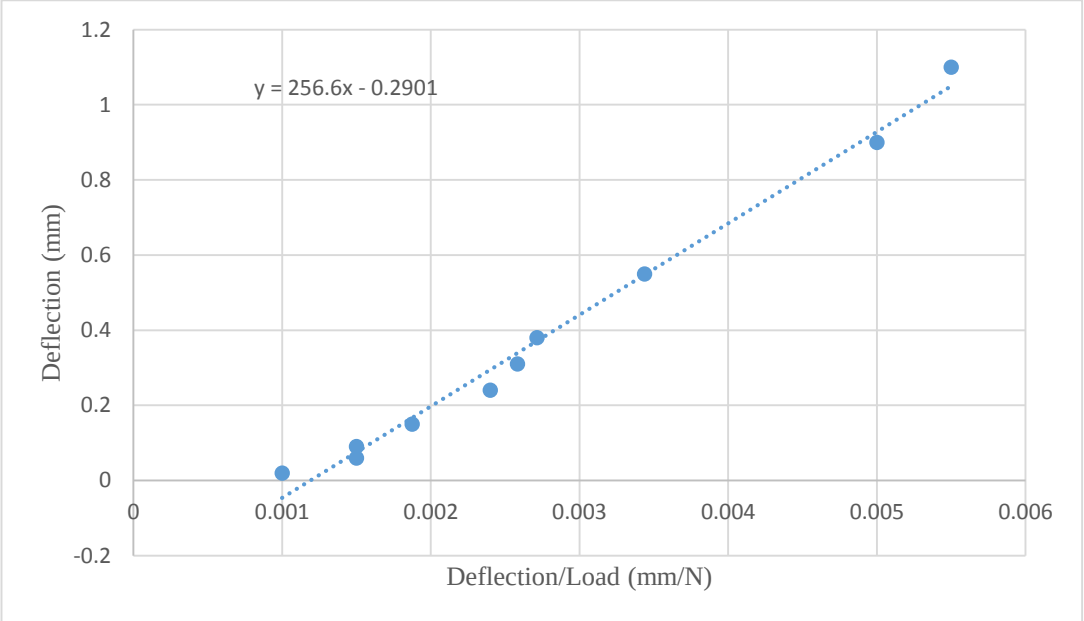

Figure 4.5 Deflection vs deflection-load ratio of $[\pm 45_B/\ 0_C/\ 0_C/\ 0_B]_s^\circ$ laminate

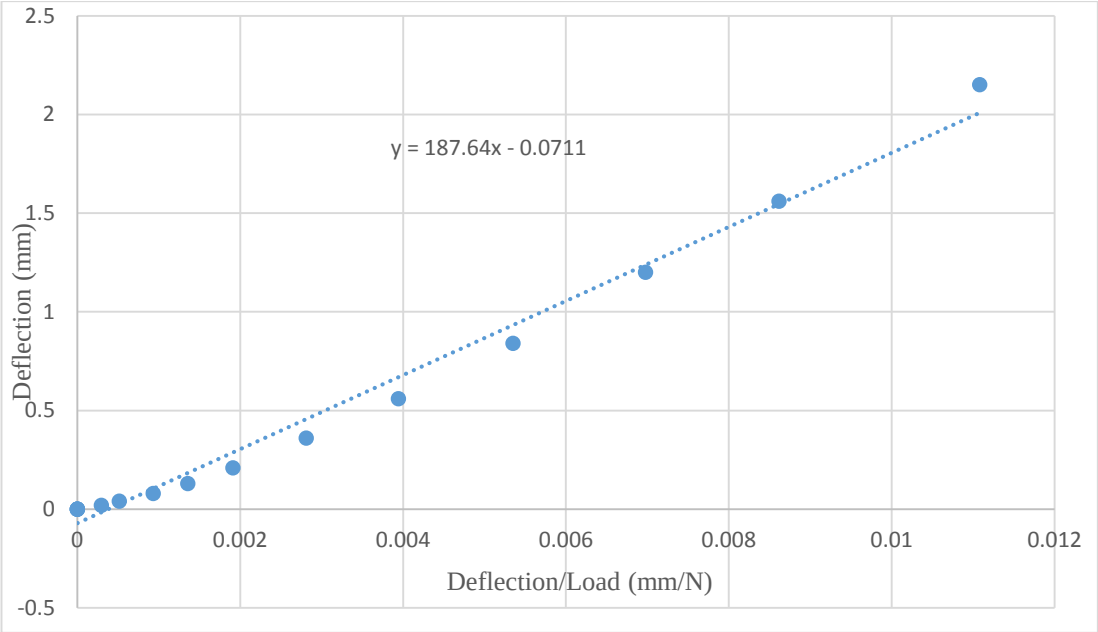

Figure 4.6 Deflection vs deflection-load ratio of $[\pm 45_B/0_B/\ 0_C/\ 0_C]_s^\circ$ laminate

4.2 NUMERICAL AND EXPERIMENTAL RESULTS COMPARISON

Nonlinear FEA results of six different laminates were compared with the experimental results. Table 4.1 shows the comparison between the numerical and experimental results and figure 4.7 shows a graphical representation of the results.

Table 4.1 Numerical and experimental critical buckling load of different stacking sequences

	Critical Buckling Load				
Stacking Sequence	Nonlinear FEA (N)	Stress, σ_{cr} (FEA) (MPa)	Experiment (N)	Stress, σ_{cr} (Exp.) (MPa)	Percentage Difference (%)
(1)$[0_B/\ 0_B/\ 0_B/\ 0_B]_s^\circ$	267	1.85	261	1.81	2
(2)$[0_C/\ 0_C/\pm 45_B\ /0_B]_s^\circ$	644	4.36	519	3.5	19
(3)$[0_C/\ 0_C/0_B/\pm 45_B]_s^\circ$	567	4.42	629	4.86	11
(4)$[0_C/\ 0_C/\ \pm 45_B/\ 0_C]_s^\circ$	697	4.40	586	3.60	18
(5)$[\pm 45_B/0_C/\ 0_C/\ 0_B]_s^\circ$	368	2.41	256	1.67	30
(6)$[\pm 45_B/0_B/\ 0_C/\ 0_C]_s^\circ$	180	1.27	188	1.33	4

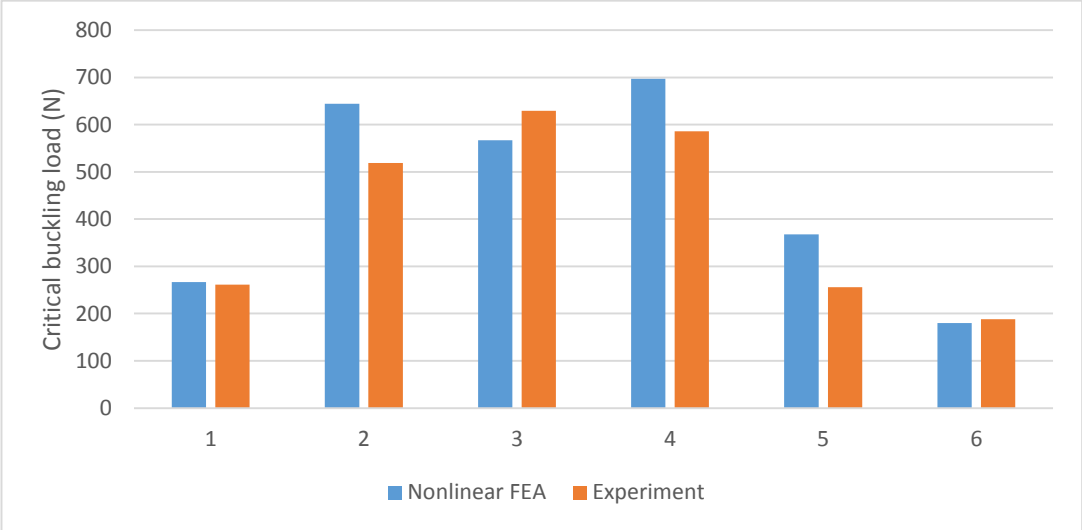

Figure 4.7 Nonlinear FEA results and experimental results comparison

The percentage difference less than 20% between the FEA results and the experimental results is considered to be acceptable [28]. Results that are shown in Table 4.1 show that all the six laminates had less than 20% percentage difference except $[\pm 45_B/\ 0_C/\ 0_C/\ 0_B]_s^\circ$ laminate which had 30% percentage difference. Several factors may contribute to the differences in the results of the FEA and the experiment such as the variation of the thickness of the real specimen, the interfacial bond between the fiber and matrix phases and fiber volume fraction. Even though, the nonlinear FEA presented in this work includes geometrical nonlinearities, high variation in the thickness of the specimen could result in some percentage error between the numerical and experimental results. The efficiency of load transfer between matrix and fiber depends on the interfacial bond. Thus, weak interfacial bond will result in low buckling load. Furthermore, the fiber volume fraction obtained from matrix ignition test was between 33% - 38%. In the FE modelling the properties of the a unidirectional lamina was calculated using rule of mixtures of composite materials and the fiber volume fraction was assumed to be 35% for all laminates. Variation on the fiber volume fractions between the real specimen and the modelled one will result in the variation of the critical buckling load between the two methods.

4.3 FINITE ELEMENT ANALYSIS RESULTS

4.3.1 Effect of Fiber Orientation

The effect of fiber orientation on the critical buckling load of a four-layer symmetric basalt/epoxy composite laminated plate was studied using nonlinear FEA. Table 4.2 shows the critical buckling loads of different fiber orientations. Figure 4.8 shows the graph of critical buckling load vs fiber orientation.

Table 4.2 Critical buckling loads of different fiber orientations

θ	**Critical Buckling Load (N)**							
	[θ/0]	**[0/θ]**	**[θ/90]**	**[90/θ]**	**[θ/30]**	**[30/θ]**	**[θ/45]**	**[45/θ]**
90	15.32	55.442	8.614	8.614	8.9048	8.815	10.017	12.703
80	15.22	55.393	8.531	8.6071	8.7664	8.7118	9.8907	12.576
70	15.016	55.301	8.431	8.561	8.4174	8.4582	9.4504	12.004
60	15.049	55.329	8.815	8.9048	8.3266	8.3266	9.0712	11.238
50	16.187	55.722	10.721	9.5333	9.5838	8.6578	9.7557	10.94
40	20.196	56.702	15.586	10.609	14.033	9.6558	13.432	11.445
30	28.975	58.256	24.238	12.047	23.136	11.235	22.077	12.922
20	42.029	60.024	36.298	13.591	36.139	13.018	35.447	14.939
10	55.578	61.447	49.206	14.833	49.257	14.463	49.399	16.777
0	62.003	62.003	55.442	15.32	55.329	14.049	56.131	17.691

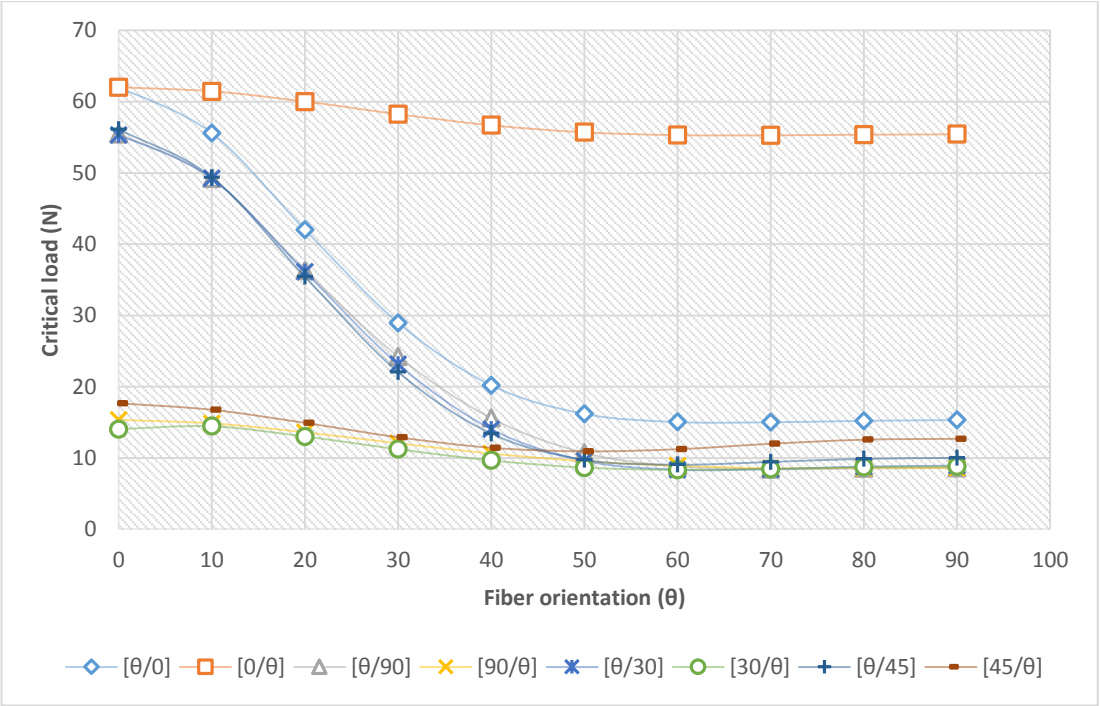

Figure 4.8 Critical buckling load vs fiber orientation

The graph shows that when the outer layer is kept constant whilst the fiber orientation of the inner layer varied from 0° - 90°, the critical buckling load does not change much. However, if the inner layer is kept constant whilst the fiber orientation of the outer layer varied from 0° - 90°, the critical buckling load decreases rapidly until θ value of 50°, after that the critical buckling load is almost constant. This indicates that the orientation of the outer layer plays more significant role on the load carrying capability of the laminate.

All stacking sequences achieved their highest critical buckling load at θ value of 0°. Moreover, the highest critical buckling load was achieved by $[0/0]_s^{\circ}$ laminate. The fiber orientation angle is measured relative to the applied load. 0°fiber orientation is parallel to the applied load. $[0/0]_s^{\circ}$ is the best fiber orientation as far as buckling strength is concerned because all layers are oriented in the load direction which enhances the buckling strength of the laminate.$[60/30]_s^{\circ}$ has the lowest critical buckling strength among all orientations.

4.3.2 Effect of Ply Stacking Sequence

The effect of ply-stacking sequence on the critical buckling load of pure basalt/epoxy, carbon/epoxy and hybrid basalt-carbon/epoxy was studied using nonlinear FEA. Table 4.3 shows the critical buckling load of those stacking sequences.

Table 4.3 Critical buckling load of pure and hybrid laminates

Group	Stacking Sequence	Critical Buckling Load (N)	Critical Stress, σ_{cr} (MPa)
Pure Laminates	$[0_B/\ 0_B/\ 0_B/\ 0_B]_s^\circ$	189	1.48
	$[0_C/\ 0_C/\ 0_C/\ 0_C]_s^\circ$	474	3.70
Hybrid Laminates with Basalt Fibers in the Inner Layers and Carbon Fibers in the Outer Layers	$[0_C/\ 0_C/\ 0_B/\pm 45_B]_s^\circ$	437	3.41
	$[0_C/\ 0_C/\pm 45_B\ /0_B]_s^\circ$	428	3.34
	$[0_C/\ 0_C/\ \pm 45_B/\ 0_C]_s^\circ$	432	3.38
Hybrid Laminates with Basalt Fibers in the Outer Layers and Carbon Fibers in the Inner Layers	$[\ 0_B/\pm 45_B/\ 0_C\ /\ 0_C]_s^\circ$	186	1.45
	$[\pm 45_B/0_B/\ 0_C/\ 0_C]_s^\circ$	132	1.03
Hybrid Laminates with Basalt Fibers Sandwiching Carbon Fibers	$[\ 0_B/\ 0_C/\ 0_C/\pm 45_B]_s^\circ$	310	2.42
	$[\pm 45_B/\ 0_C/\ 0_C\ /\pm 45_B]_s^\circ$	216	1.69
	$[\pm 45_B/\ 0_C/\ 0_C/\ 0_B]_s^\circ$	221	1.73

Each of the four groups shown in Table 4.3 will be discussed in section **4.3.2.1** through section **4.3.2.4**.

4.3.2.1 Pure Laminates

First the buckling behaviour of pure basalt reinforced epoxy was compared with pure carbon reinforced epoxy. Table 4.4 shows the critical buckling load of the two laminates.

Table 4.4 Critical buckling load of pure basalt and pure carbon reinforced epoxy

Stacking Sequence	**Critical Buckling Load (N)**	**Critical Stress, σ_{cr} (MPa)**
$[0_B/\ 0_B/\ 0_B/\ 0_B]_s^\circ$	189	1.48
$[0_C/\ 0_C/\ 0_C/\ 0_C]_s^\circ$	474	3.70

The critical buckling load of pure carbon fibers reinforced epoxy oriented in 0° direction is higher than the critical buckling load of basalt fibers reinforced epoxy oriented in the same direction. That is due to the high longitudinal stiffness of carbon fibers.

4.3.2.2 Hybrid Laminates With Basalt Fibers in The Inner Layers and Carbon Fibers in The Outer Layers

In this section, basalt-carbon/epoxy hybrid laminates were studied. The outer layers were reinforced with carbon fibers while the inner layers were reinforced with basalt fibers. Table 4.5 illustrates the critical buckling load of three different stacking sequences.

Table 4.5 Critical buckling loads of hybrid laminates with basalt fibers in the inner layers and carbon fibers in the outer layers

Stacking Sequence	Critical Buckling Load (N)	Critical Stress, σ_{cr} (MPa)
$[0_C/\ 0_C/\ 0_B/\pm 45_B]_s^\circ$	437	3.41
$[0_C/\ 0_C/\pm 45_B\ /0_B]_s^\circ$	428	3.34
$[0_C/\ 0_C/\ \pm 45_B/\ 0_C]_s^\circ$	432	3.38

Hybrid laminates with four carbon fibers reinforcement layers oriented in the 0° direction in the outer surface and four basalt fibers reinforced layers in the inner surface have high critical buckling loads. The critical buckling loads of those laminates are even comparable to that of pure carbon fibers reinforcement. That is due to the fact that the outer layers carry most of the buckling load. The critical buckling load of $[0_C/\ 0_C/\ 0_B/\pm 45_B]_s^\circ$ laminate is higher than the critical buckling load of $[0_C/\ 0_C/\ \pm 45_B/\ 0_C]_s^\circ$ laminate despite the fact that $[0_C/\ 0_C/\ \pm 45_B/\ 0_C]_s^\circ$ laminate has six carbon fibers reinforced layers, two of them are in the innermost surface of the laminate and four in the outermost surface, compared to only four carbon fiber layers in the $[0_C/\ 0_C/\ 0_B/\pm 45_B]_s^\circ$ at the outermost surface. The reason is that the third layer of $[0_C/\ 0_C/\ 0_B/\pm 45_B]_s^\circ$ laminate is oriented in the 0°direction compared to the $\pm 45^\circ$ in $[0_C/\ 0_C/\ \pm 45_B/\ 0_C]_s^\circ$ laminate. $[0_C/\ 0_C/\pm 45_B\ /0_B]_s^\circ$ laminate has the lowest buckling strength among the three laminates. $[0_C/\ 0_C/\ 0_B/\pm 45_B]_s^\circ$ laminate is the best optimized stacking sequence among the three.

4.3.2.3 Hybrid Laminates With Basalt Fibers in The Outer Layers and Carbon Fibers in The Inner Layers

Table 4.6 shows the critical buckling loads of two ply-stacking sequences of hybrid laminates. Both laminates have four basalt fibers reinforcement in the outer layers and four carbon fibers reinforcement in the inner layers.

Table 4.6 Critical buckling load of hybrid laminates with basalt fibers in the outer layers and carbon fibers in the inner layers

Stacking Sequence	Critical Buckling Load (N)	Critical Stress, σ_{cr} (MPa)
$[\,0_B/\pm 45_B/\,0_C\,/\,0_C]_s^\circ$	186	1.45
$[\pm 45_B/0_B/\;0_C/\,0_C]_s^\circ$	132	1.03

The results show that reinforcing the outer layers with basalt fibers and the inner layers with carbon fibers results in a very low buckling strength. That is due to the fact the Basalt fibers has lower longitudinal modulus of elasticity than that of carbon fibers and the outer layers are the most critical in the buckling strength of composite laminates. The buckling strength of $[\,0_B/\pm 45_B/\,0_C\,/\,0_C]_s^\circ$ laminate is higher than the buckling strength of $[\pm 45_B/0_B/\;0_C/\,0_C]_s^\circ$ laminate, because the reinforcement in the outer layer is oriented in the 0° direction.

4.3.2.4 Hybrid Laminates With Basalt Fibers Sandwiching Carbon Fibers

The results of buckling strength of hybrid laminates featuring basalt fibers reinforcement in the outer and inner layers and carbon fibers in the middle layers are presented in this section. Table 4.7 shows the critical buckling loads of those laminates.

Table 4.7 Critical buckling load of hybrid laminates with basalt fibers sandwiching carbon fibers

Stacking Sequence	Critical Buckling Load (N)	Critical Stress, σ_{cr} (MPa)
$[\,0_B/\,0_C/\;0_C/\pm 45_B]_s^\circ$	310	2.42
$[\pm 45_B/\,0_C/\,0_C\,/\pm 45_B]_s^\circ$	216	1.69
$[\pm 45_B/\,0_C/\;0_C/\,0_B]_s^\circ$	221	1.73

Results presented in Table 4.7 show that placing one basalt reinforcement in the outer layer followed by carbon reinforced layers increases the buckling strength of the

laminate by around 60% compared to placing the carbon fiber reinforcements in the innermost layers. $[\,0_B/\,0_C/\;0_C/\pm 45_B]_s^{\circ}$ sustained the highest buckling load among the three stacking sequences because the outer layers are oriented in the 0° direction.

CHAPTER 5

CONCLUSION AND RECOMMENDATIONS

5.1 CONCLUSION

The effect of fiber orientation and ply stacking sequence on the critical buckling load of a symmetric basalt/epoxy and basalt-carbon/epoxy composite laminates were studied. The laminates were subjected to simply supported boundary conditions and axial compressive load. Nonlinear FEA using ANSYS software was used. FEA results were validated by experimental results of six different hybrid laminates. FEA results had good agreement with the experimental results with percentage difference less than 20% in most laminates.

Results of the nonlinear FEA on the effect of fiber orientation on the critical buckling load of four-layer symmetric basalt/epoxy laminates showed that:

1. The outer layer plays the most significant role in the load carrying capability of the composite laminate.
2. The critical buckling load of the composite laminate decreases continuously when the orientation of the outer layer is varied from $0^{\circ} - 90^{\circ}$ until θ value of 50°. After 50° the critical buckling load is almost constant.
3. The critical buckling load does not change much if the outer layer is kept constant regardless of the orientation of the inner layer.
4. Laminates having 0° fiber orientation in the outer layer had the highest critical buckling loads.
5. $[0/0]_s^{\circ}$ laminate sustained the highest critical buckling load.
6. $[60/30]_s^{\circ}$ laminate had the lowest critical buckling load.

Nonlinear FEA of hybrid basalt-carbon/epoxy showed that:

1. Laminates having carbon fibers reinforcement in the outer layers sustained higher load compared with laminates reinforced with basalt fibers in the outer layers.

2. $[0_C/\ 0_C/\ 0_B/\pm 45_B]_S^{\circ}$ laminate is the best optimization for buckling strength among all hybrid laminates.

5.2 RECOMMENDATIONS

Hybrid stacking sequences that were studied in the present work are of great concern for wind turbines industry. The common fibers that are used nowadays are glass fibers and carbon fibers. A future continuation of this work would be to compare the performance of basalt-carbon/epoxy with glass-carbon/epoxy hybrid laminates.

REFERENCES

[1] Campbell, F. C., 2010,"Structural composite materials,": *ASM international*.

[2] Heidari-Rarani, M., Khalkhali-Sharifi, S. S. and Shokrieh, M. M., 2014," Effect of ply stacking sequence on buckling behavior of E-glass/epoxy laminated composites," *Computational Materials Science* **89:** 89-96

[3] Alam, S. H., Habib, F., Irfan, M., Iqbal, W. and Khalid, K., 2010. "Effect of orientation of glass fiber on mechanical properties of GRP composites," *J. Chem. Soc. Pak* **32 (3):** 265

[4] Bai, J. and Xiong, J., 2014, "Temperature effect on buckling properties of ultra-thin-walled lenticular collapsible composite tube subjected to axial compression," *Chinese Journal of Aeronautics* **27(5):** 1312-1317

[5] Shukla, K. K., Nath, Y., Kreuzer, E. and Kumar, K. V., 2005, "Buckling of laminated composite rectangular plates," *Journal of aerospace engineering* **18 (4):** 215-223

[6] Topal, U. and Uzman, Ü., 2009, "Effects of nonuniform boundary conditions on the buckling load optimization of laminated composite plates," *Materials & Design* **30 (3):** 710-717

[7] SudhirSastry, Y. B., Budarapu, P. R., Madhavi, N. and Krishna, Y., 2015, "Buckling analysis of thin wall stiffened composite panels," *Computational Materials Science* **96:** 459-471

[8] Guo, M. W., Harik, I. E. and Ren, W. X., 2002, "Buckling behavior of stiffened laminated plates," *International journal of solids and structures **39*** **(11):** 3039-3055

[9] Short, G. J., Guild, F. J. and Pavier, M. J., 2002, "Delaminations in flat and curved composite laminates subjected to compressive load," *Composite Structures* **58 (2):** 249-258

[10] Arman, Y., Zor, M. and Aksoy, S., 2006, "Determination of critical delamination diameter of laminated composite plates under buckling loads," *Composites science and technology* **66 (15):** 2945-2953

[11] Yeter, E., Erkliğ, A. and Bulut, M., 2014, "Hybridization effects on the buckling behavior of laminated composite plates," *Composite Structures* **118:** 19-27

[12] Hu, H. T., Yang, C. H. and Lin, F. M., 2006, "Buckling analyses of composite laminate skew plates with material nonlinearity," *Composites Part B: Engineering* **37 (1):** 26-36

[13] Erkliğ, A., Yeter, E. and Bulut, M., 2013, "The effects of cut-outs on lateral buckling behavior of laminated composite beams," *Composite Structures* **104:** 54-59

[14] Ni, Q. Q., Xie, J. and Iwamoto, M., 2005, "Buckling analysis of laminated composite plates with arbitrary edge supports," *Composite structures* **69 (2):** 209-217

[15] Park, J. H., Hwang, J. H., Lee, C. S. and Hwang, W., 2001, "Stacking sequence design of composite laminates for maximum strength using genetic algorithms," *Composite Structures* **52(2):** 217-231

[16] Topal, U. and Uzman, Ü, 2008, "Thermal buckling load optimization of laminated composite plates," *Thin-Walled Structures* **46 (6):** 667-675

[17] Özben, T., 2009, "Analysis of critical buckling load of laminated composites plate with different boundary conditions using FEM and analytical methods," *Computational Materials Science* **45 (4):** 1006-1015

[18] Cagdas, I. and Adali, S., 2010, "Design of a laminated composite variable curvature panel under uniaxial compression," *Engineering Computations **29** **(1):*** 48-64

[19] Geier, B., Meyer-Piening, H. R. and Zimmermann, R., 2002, "On the influence of laminate stacking on buckling of composite cylindrical shells subjected to axial compression," *Composite structures* **55 (4):** 467-474

[20] Topal, U., 2011, "Application of Layerwise Optimization Method to Maximum Buckling Load Design of Laminated Thin Plates," In *Proceedings of 6th International Advanced Technologies Symposium* **11:** 16-18

[21] Chen, T. L. and Bert, C. W., 1976, "Design of composite-material plates for maximum uniaxial compressive buckling load," In *Proc. Okla. Acad. Sci **56:*** 104-107

[22] Jadhav, M. M. and Gunjavate, P. V., 2012, "Optimization of buckling load for glass fiber composite laminate by using ansys," *International Journal of Advanced Engineering Research and Studies* **2 (1):** 144-147

[23] Eker A. A. and Eker B. (2013). General Assessment of Fıber - Reınforced Composıtes Selectıon in Wınd Turbıne Blades, Recent Advances in Composite Materials for Wind Turbines Blades, Dr. Brahim Attaf (Ed.), ISBN 978-0-9889190-0-6,WAP-AMSA,Availablefrom: http://www.academicpub.org/amsa/chapterInfo.aspx

[24] Boni, L., Fanteria, D. and Lanciotti, A., 2012, "Post-buckling behaviour of flat stiffened composite panels: Experiments vs. analysis," *Composite Structures* **94 (12):** 3421-3433

[25] Gal, E., Levy, R., Abramovich, H. and Pavsner, P., 2006, "Buckling analysis of composite panels," *Composite structures* **73 (2):** 179-185

[26] ANSYS Procedures. Engineering analysis system verification manual, vol. 1. Houston (PA, USA): Swanson Analysis System, Inc.; 1993.

[27] Mengal, A. N., Karuppanan, S., and Wahab, A. A., 2014, "Structural Analysis of Basalt Fiber Reinforced Plastic Wind Turbine Blade," *MATEC Web of Conferences* **13:** 04019

[28] Pineda, E. J., Meyers, D. E., Kosareo, D. N., Zalewski, B. F. and Dixon, G. D., 2013, "Buckling Testing and Analysis of Honeycomb Sandwich Panel Arc Segments of a Full-Scale Fairing Barrel. Part 2; 6-Ply In-Autoclave Facesheets,"

APPENDICES

APPENDIX A: ANSYS Command Code for Buckling Analysis

```
/PREP7
UIMP,1,EX,EY,EZ,37700e6,5237e6,5237e6
UIMP,1,GXY,GYZ,GXZ,2050e6,3630e6,3630e6
UIMP,1,PRXY,PRYZ,PRXZ,0.2,0.21,0.21
ET,1,Shell281
SECTYPE,1,SHELL
SECDATA,0.0005,1,90
SECDATA,0.0005,1,90
SECDATA,0.0005,1,90
SECDATA,0.0005,1,90
RECTNG,0,0.04,0,0.40
ESIZE,0.01
AMESH,all
FINISH
/SOLU
ANTYPE,STATIC
PSTRES,ON
D,1,UZ,0
D,2,UZ,0
D,3,UZ,0
D,4,UZ,0
D,5,UZ,0
```

D,6,UZ,0

D,7,UZ,0

D,8,UZ,0

D,9,UZ,0

D,1,UX,0

D,2,UX,0

D,3,UX,0

D,4,UX,0

D,5,UX,0

D,6,UX,0

D,7,UX,0

D,8,UX,0

D,9,UX,0

D,10,UZ,0

D,90,UZ,0

D,91,UZ,0

D,92,UZ,0

D,93,UZ,0

D,94,UZ,0

D,95,UZ,0

D,96,UZ,0

D,97,UZ,0

D,10,UX,0

D,90,UX,0

D,91,UX,0

D,92,UX,0

D,93,UX,0

D,94,UX,0

D,95,UX,0

D,96,UX,0

D,97,UX,0

D,10,UY,0

D,90,UY,0

D,91,UY,0

D,92,UY,0

D,93,UY,0

D,94,UY,0

D,95,UY,0

D,96,UY,0

D,97,UY,0

F,6,FY,1

SOLVE

FINISH

/SOLU

ANTYPE,BUCKLE

BUCOPT,LANB,10

SOLVE

FINISH

/solu

Expass

Mxpand

Solve

finish